RSC Advances

PAPER

View Article Online
View Journal | View Issue

Cite this: *RSC Adv.*, 2021, **11**, 17704

High performance polypyrrole/SWCNTs composite film as a promising organic thermoelectric material

Zhaohua Liu,†[a] Jiye Sun,†[a] Haijun Song,*[a] Yicheng Pan,[a] Yufei Song,[a] Yuehong Zhu,[a] Yuanyuan Yao,*[b] Fengli Huang[a] and Chuncheng Zuo*[a]

Conducting polymer thermoelectric (TE) materials have received great attention due to their unique properties. In this work, polypyrrole (PPy)/single-walled carbon nanotubes (SWCNTs) composite films with improved TE performance have been prepared by chemical interfacial polymerization at the cyclohexane/water interface under a controlled temperature. Attributed to the smooth surface, higher conjugation length and more ordered molecular structure of the interfacial polymerized PPy film, the electrical conductivity can be as high as ~500 S cm^{-1}. To further enhance the TE properties of PPy, SWCNT was added to construct a PPy/SWCNTs composite. Due to the synergistic effect between the two phases and the energy filtering effect at the interfaces between PPy and SWCNTs, the Seebeck coefficient of the composite enhanced significantly with the increase SWCNTs content. The composite shows an optimal power factor of 37.6 ± 2.3 μW mK^{-2} when the content of SWCNTs is 0.8 mg. This value is one of the largest values among the reported PPy based composites fabricated by the chemical polymerization method. The results indicate that interfacial polymerization under a controlled temperature is a promising way to improve the TE performance of conducting polymer based composite materials.

Received 8th April 2021
Accepted 10th May 2021

DOI: 10.1039/d1ra02733f

rsc.li/rsc-advances

Introduction

Thermoelectric (TE) energy conversion technology which can directly convert heat into electrical energy in a reliable and eco-friendly manner is regarded as a new energy generation technology to realize the recycling of waste heat.[1–3] The conversion efficiency of TE materials is determined by the dimensionless figure of merit, $ZT = S^2\sigma T/\kappa$, where σ is the electrical conductivity, S is the Seebeck coefficient, κ is the thermal conductivity, T is the absolute temperature, and $S^2\sigma$ is the power factor, respectively. Traditional inorganic semiconductors, such as Bi_2Te_3, PbTe, and SnSe are the most widely used TE materials due to their high TE power factor.[4–6] However, the high cost, difficulty of processing, and scarcity of their raw materials limit their wide application.

In recent years, organic materials, especially conducting polymers have attracted increasing attention as a new type of TE material owing to their unique superiorities, such as lightweight, abundance resource, easy synthesis, and low thermal conductivity.[7–12] Typical conducting polymers, such as polyaniline (PANi) and poly(3,4-ethylenedioxythiophene) (PEDOT) are the most extensively investigated organic TE materials for their tuneable electrical conductivity and Seebeck coefficient, and some reported TE performances even can comparable to that of the Bi_2Te_3 at room temperature. For example, through optimizing the oxidation level of PEDOT:tosylate film, a maximum power factor of 324 μW mK^{-2} has been obtained with a ZT value of 0.25;[11] the PEDOT/Bi_2Te_3 hybrid films with monodispersed and periodic Bi_2Te_3 nanophase showed a power factor as high as ~1350 μW mK^{-2} with a ZT of 0.58 at room temperature;[13] the PANi/graphene/PANi/CNT composites with an ordered molecular structure showed a power factor of 1825 μW mK^{-2};[14] the PANi/SWCNTs composite films with a highly ordered structure showed a power factor of 217 μW mK^{-2}.[15]

Among various conducting polymers, polypyrrole (PPy) has been used in the field of biosensors, flexible batteries, solid electrolytic capacitors *etc.* due to its excellent properties, such as ease of synthesis, chemical stability, relative environmental stability, and biocompatibility.[16–19] Also, the TE properties of PPy has been studied, however, the conductivity of the PPy prepared by ordinary chemical/electrochemical polymerization is generally very low, in the range of 10^{-3} to 10^{1} S cm^{-1},[20–22] which has resulted in low TE properties when compared with other conducting polymers like PEDOT and PANi. For example, Bharti *et al.*[23] have prepared flexible PPy/Ag nanocomposite films through a photo-polymerization process, and the electrical conductivity of the composite films increased from 1.5 (pure PPy) to 17.3 S cm^{-1} with the addition of Ag particles,

[a]College of Mechanical and Electrical Engineering, Jiaxing University, Jiaxing 314001, PR China. E-mail: songhaijun8837@126.com; zuocc@mail.zjxu.edu.cn

[b]College of Biological, Chemical Sciences and Engineering, Jiaxing University, Jiaxing 314001, PR China. E-mail: yaoyuanyuan2007@163.com

† These authors contributed equally to this work.

although the enhancement is significant, the electrical conductivity is still too low to meet the TE application. Wang *et al.*[24] synthesized PPy/multi-walled carbon nanotubes (MWCNT) composite powders, and due to the enhanced electrical conductivity and Seebeck coefficient, an optimized of power factor of 2.079 μW mK^{-2} has been obtained, which is about 26 times as high as that of pure PPy, but the value is still far from satisfactory. Chen's group has made some effort to enhance the TE properties of PPy.[25–28] In 2014 they prepared reduced graphene oxide (rGO)/PPy composites using a template-directed *in situ* polymerization method, the composite showed an 84 times enhancement of power factor compared than that of pure PPy, while its value is still too low (3.01 μW mK^{-2}), which is mainly caused by the low electrical conductivity of pure PPy (3.97 S cm^{-1}).[25] Recently, they have discussed the relationship between PPy nanostructure morphology and TE performance and found that the straight PPy nanowires displayed a high electrical conductivity of 221.7 S cm^{-1} with a power factor of 22.6 μW mK^{-2}.[27] Therefore, to improve the TE properties of PPy by tuning its electrical conductivity seems to be an effective approach.

Interfacial polymerization method has been proved to be an effective way to enhance the electrical conductivity of PPy, especially under a low temperature.[29,30] However, high conductive PPy film obtained under low temperature is usually wrinkled and it's hard to get flat film with large-area. And except for high electrical conductivity, an excellent TE performance should also process Seebeck coefficient. SWCNTs have been proved to be an effective filler to improve the TE properties of conducting polymer by enhancing the Seebeck coefficient of the composite.[31–33] Compared with traditional inorganic crystals, CNTs are non-toxic, lightweight and show good mechanical strength, high electrical conductivity. And the large aspect ratio of CNTs has made them effective conductive fillers in polymers. Therefore, in this study, high conductive PPy/SWCNTs composite films are prepared by chemical interfacial polymerization at the interface of cyclohexane/water under a controlled temperature. By altering the content of SWCNTs in the composite, the film shows a highest power of 37.6 μW mK^{-2}, which is among the largest value for PPy and its composites reported so far. This study provides a new way to optimize the TE performance of PPy based materials and also this method can be applied to prepare other kinds of conducting polymer TE materials.

Experimental

Materials

Pyrrole (chemical pure grade, purity ≥ 98.0%), *p*-toluenesulfonic acid (PTSA, analytical reagent grade), $FeCl_3$, cyclohexane, and ethanol were obtained from Sinopharm Chemical Reagent Co., Ltd. SWCNTs (diameter: 1–2 nm, length 5–30 μm, purity ≥ 95%) synthesized by a chemical vapor deposition method were purchased from Chengdu Organic Chemicals Co. Ltd., Chinese Academy of Sciences (Chengdu, China). All the reagents were used as received in the preparation procedure without further purification.

Synthesis of PPy/SWCNTs composite film through an interfacial polymerization

The prepare procedure of PPy/SWCNTs composite film is described schematically in Fig. 1. The synthetic procedure is conducted at a cyclohexane/water interface with pyrrole monomer in organic phase while $FeCl_3$ and PTSA in aqueous phase. First, 12 mL aqueous solution containing 0.36 M $FeCl_3$ and 0.36 M PTSA was added into a Petri dish (solution A) and placed in a 8 °C freezer 1 h for pre-cooled treatment. Then, 12 mL cyclohexane containing 0.036 M pyrrole and different amounts of SWCNTs was added drop by drop to the aqueous solution. A clear interface between cyclohexane and aqueous solutions is formed. The polymerization was processed at 8 °C statically for 30 min in freezer. Finally, a thin and dark composite film was formed at the interface. The film was rinsed with deionized water and absolute ethanol in sequence for 3 times, then transferred to a glass substrate (2 × 2 cm^2) and dried in vacuum at 70 °C for 12 h. Pure PPy film was prepared by the same method without the addition of SWCNTs.

Also, *in situ* polymerized PPy powder was prepared as a comparison, and the preparation procedure is as follow. 0.36 M $FeCl_3$ and 0.36 M PTSA was dissolved in 50 mL distilled water under 8 °C. Then 0.036 M pyrrole monomer was slowly added into the above solution and stirred for 24 h. The obtained precipitates were collected by centrifugation and rinsed with deionized water and absolute ethanol in sequence for 3 times. Finally, the black powder was collected after being dried under vacuum at 70 °C for 12 h.

Measurements and characterizations

Electrical conductivity and Seebeck coefficient of the samples were measured simultaneously in a vacuum atmosphere on a MRS-3 thin-film thermoelectric test system (Wuhan Giant Instrument Technology Co., Ltd). The morphology of the films was measured by field-emission scanning electron microscopy (FESEM, Hitachi, S-4800). Fourier transform infrared (FT-IR) spectroscopy of the samples were obtained from a Fourier infrared spectrometer (Thermo 470 FT-IR). Raman spectroscopy was performed using a WITech CRM 200 Raman spectrometer (excitation wavelength: 632.8 nm). The thickness of the films was obtained from a step profiler (BRUKER, DEKTAK XT).

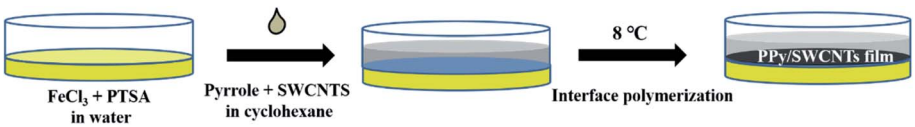

Fig. 1 Schematic illustration of the procedure to prepare PPy/SWCNTs composite film.

Results and discussion

The typical SEM images of the samples are shown in Fig. 2. The PPy powder prepared by traditional chemical polymerization in Fig. 2A shows a cauliflower-like morphology made up of nanoparticles with diameter about 20–30 nm. While, the PPy film prepared by chemical interfacial polymerization at a low temperature displays a very smooth, uniform and compact surface, as shown in Fig. 2B. It is well known that a compact and smooth surface can facilitate the electron transfer of π-conjugated polymers, and hence contributes to a high electrical conductivity. For the PPy/SWCNTs (0.3 mg, Fig. 2C) composite film, the SWCNTs distributed randomly in the PPy matrix, and a sparse SWCNTs conductive network is formed. With the enhancement of SWCNTs content, the conductive network becomes dense. And the formation of the SWCNTs conductive network is believed to be beneficial to the enhancement of TE performance of the composite films due to its high electronic carrier mobility and an energy filtering effect between the nanotubes and polymer layer. However, with a high SWCNTs content, some of SWCNTs self-aggregate to bundles due to van der Waals force between the SWCNTs (as shown in Fig. 2E) and these bundles may destroy the continuity and integrity of PPy film and lead to a low electrical conductivity of the composite films.

The chemical composition of the prepared PPy and PPy/SWCNTs composite has been characterized by FT-IR spectra in Fig. 3. All the results display very similar spectra, which are identical to the characteristic absorption bands reported for PPy,[34,35] indicating successful synthesis of PPy by both methods. The strong peaks at 1535 and 1446 cm^{-1} are assigned to the anti-symmetric and symmetric stretching modes of pyrrole ring, respectively; and the peaks at 1295 and 1038 cm^{-1} correspond to the C–N stretching vibration and C–H in-plane deformation vibration; the peaks at 1147 cm^{-1} is attributed to the breathing vibration of the pyrrole ring. FTIR characterization can be used to obtain qualitative and semi-quantitative information on the conjugation length of polymers. And it has already been reported that the integrated absorption area ratio (A_{1535}/A_{1446}) is

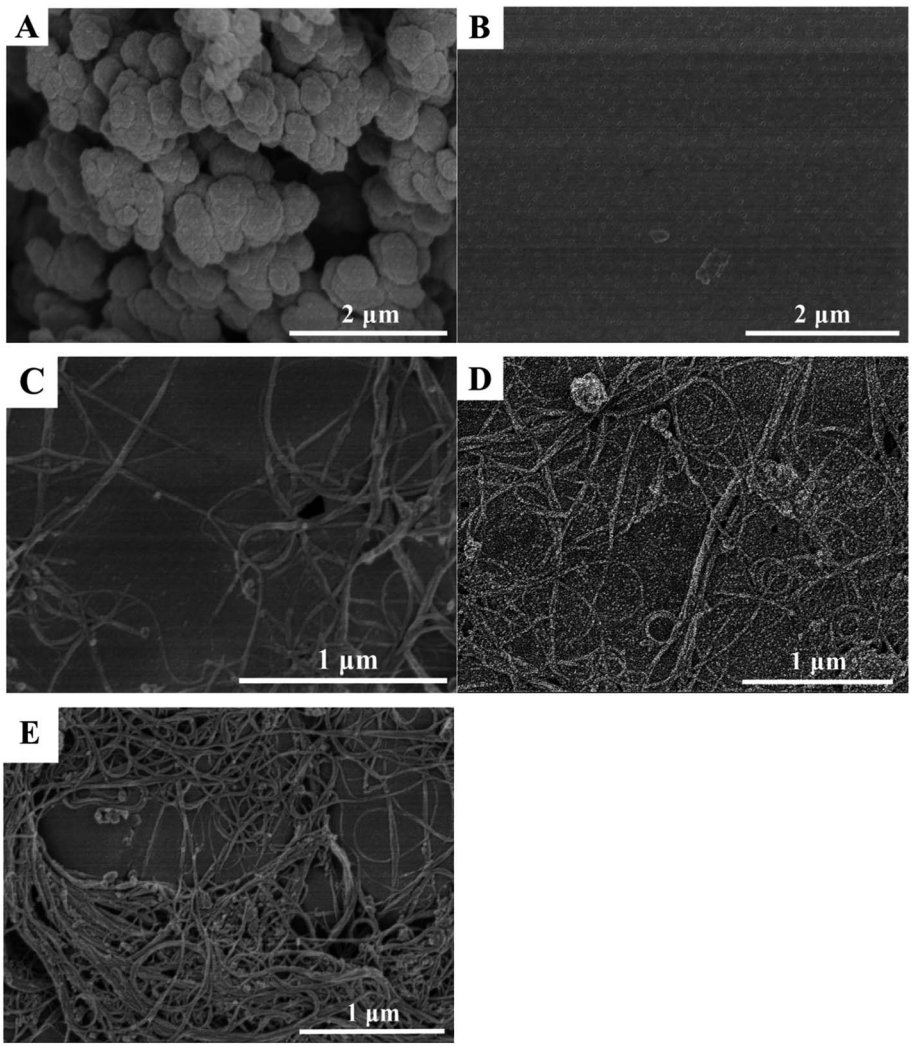

Fig. 2 FE-SEM images of the prepared samples: *in situ* polymerized PPy powder (A); interfacial polymerized PPy film (B); interfacial polymerized PPy/SWCNTs (0.3 mg) composite film (C); interfacial polymerized PPy/SWCNTs (0.5 mg) composite film (D); interfacial polymerized PPy/SWCNTs (0.8 mg) composite film (E).

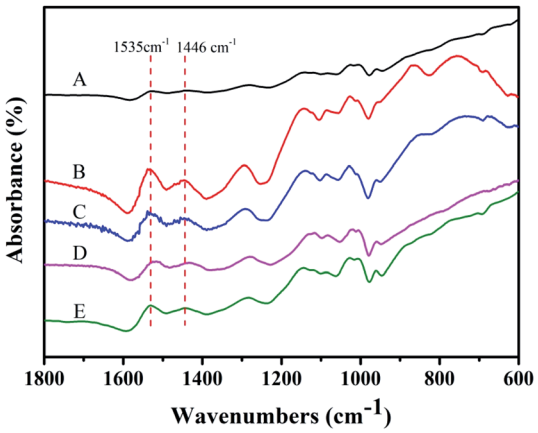

Fig. 3 FTIR spectra of the prepared samples: *in situ* polymerized PPy powder (A); interfacial polymerized PPy film (B); interfacial polymerized PPy/SWCNTs (0.3 mg) composite film (C); interfacial polymerized PPy/SWCNTs (0.5 mg) composite film (D); interfacial polymerized PPy/SWCNTs (0.8 mg) composite film (E).

inversely proportional to the conjugation length of PPy.[29,36,37] Therefore, the area ratios of the two bands (A_{1535}/A_{1446}) are calculated. For the *in situ* polymerized PPy powder, the intensity ratio I_{1535}/I_{1446} is 2.05, and the interfacial polymerized PPy film shows a value of 2.11, indicating an enhanced conjugation of the interfacial polymerized PPy film. Besides, the spectra of PPy/SWCNTs composite show a slight shift, which may be caused by the interactions between SWCNTs and PPy.

Fig. 4 shows the Raman spectra of all the samples. Several strong and similar PPy characteristic peaks were observed, peaks at 930 and 962 cm^{-1} are caused by the polaron (NH^+) and bipolaron structures (N^+) of PPy,[38] peak at1053 cm^{-1} is attributed to the neutral species in PPy, 1245 cm^{-1} is associated with antisymmetric in plane bending, 1323 cm^{-1} corresponds to C–C

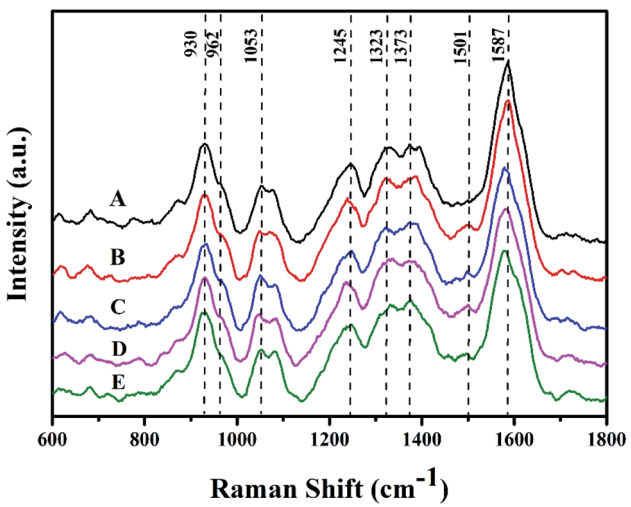

Fig. 4 Raman spectra of the prepared samples: *in situ* polymerized PPy powder (A); interfacial polymerized PPy film (B); interfacial polymerized PPy/SWCNTs (0.3 mg) composite film (C); interfacial polymerized PPy/SWCNTs (0.5 mg) composite film (D); interfacial polymerized PPy/SWCNTs (0.8 mg) composite film (E).

in ring and CC inter-ring stretching, 1373 cm^{-1} corresponds to antisymmetric in ring C–N stretching, 1499 cm^{-1} corresponds to C=C and C–N stretching, and 1587 cm^{-1} corresponds to C–C inter ring stretching in the PPy, respectively. Besides, the ratio from 1587/1501 can be used to determine the relative conjugation length.[39] For the interfacial polymerized PPy film, the value of I_{1587}/I_{1501} is 2.1, and the *in situ* polymerized PPy powder shows a value of 1.6, indicating the lengthening of the π conjugation of the PPy chains in the interfacial polymerized PPy films, which can promote the mobility of carriers. Also, compared with the pure PPy powder and film, the peaks at 1587 cm^{-1} in PPy/SWCNTs composite films present a small displacement to the low frequency, which can be attributed to the enhanced electron delocalization caused by the strong π–π conjugated interactions between SWCNTs and the PPy.[39,40] During the polymerization, the π–π interaction between two phases can induce PPy to grow along the surface of the SWCNTs, and lead to a more expanded molecular conformation and more ordered PPy chain packing, which will promote the carrier mobility in the composite.[25,41]

The TE properties of all the samples are displayed in Fig. 5. The *in situ* polymerized PPy powder shows an electrical conductivity of 10.3 ± 0.4 S cm^{-1}, with Seebeck coefficient of 6.8 ± 0.3 μV K^{-1}, and the calculated power factor is 4.8 ± 0.6 × 10^{-2} μW mK^{-2}. The electrical conductivity of interfacial polymerized PPy film can be as high as 485.7 ± 7 S cm^{-1}, with a similar Seebeck coefficient of 6.3 ± 0.3 μV K^{-1}. Due to the greatly enhanced electrical conductivity, the power factor is 1.93 ± 0.2 μW mK^{-2}, which is about 40 times larger than that of *in situ* polymerized PPy powder. After the addition of SWCNTs, the Seebeck coefficient of the obtained PPy/SWCNTs composites show a significant tendency of increase, and the value increase from 15.9 ± 0.5 μV K^{-1} for the composite contained 0.3 mg SWCNTs to 37.1 ± 1.1 μV K^{-1} when the sample contained 0.8 mg SWCNTs. This phenomenon can be attributed to the following points: (1) the synergistic effect in the composite, the composite can combines the high electrical conductivity of interfacial polymerized PPy film and the decent Seebeck coefficient of SWCNTs (~52 ± 1.6 μV K^{-1}); (2) the carrier energy filtering at the interface between PPy and SWCNT. The reported work functions of PPy and SWCNTs are 4.95 eV and 4.8 eV,[42,43] therefore, the energy barrier at the PPy/SWCNTs interface is 0.15 eV. This energy barrier can scatter low-energy carriers and allow high-energy carriers to cross over the interface. So the Seebeck coefficient is significantly increased. Although the Seebeck coefficient of the composite increase with the increased SWCNTs content, the electrical conductivity of composite decrease with the increased SWCNTs content due to the lower electrical conductivity of SWCNTs (~180 ± 3.3 S cm^{-1}). Also the agglomeration of SWCNTs may destroy the continuity of PPy film and lead to low electrical conductivity (see Fig. 2E). Finally, an optimized power factor of 37.6 ± 2.3 μW mK^{-2} has obtained for the composite contained 0.8 mg SWCNTs. Then we compared the TE properties of interfacial polymerized PPy/SWCNTs composite films prepared in this work with those in recent related studies. As shown in Table 1, the highest power factor of 37.6 ± 2.3 μW mK^{-2} in our work is superior even

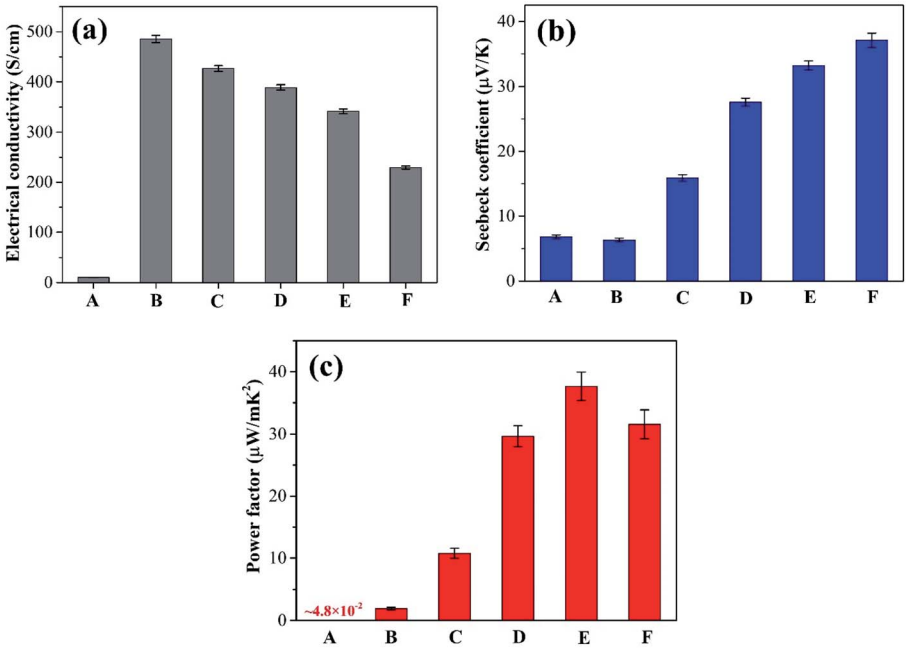

Fig. 5 Electrical conductivity (a), Seebeck coefficient (b) and power factor (c) of the prepared samples: *in situ* polymerized PPy powder (A); interfacial polymerized PPy film (B); interfacial polymerized PPy/SWCNTs (0.3 mg) composite film (C); interfacial polymerized PPy/SWCNTs (0.5 mg) composite film (D); interfacial polymerized PPy/SWCNTs (0.8 mg) composite film (E); interfacial polymerized PPy/SWCNTs (1 mg) composite film (F).

Table 1 Comparison of the TE performance of PPy based materials

Materials	Methods	Electrical conductivity (S m^{-1})	Seebeck coefficient (μV K^{-1})	Power factor (μW mK^{-2})	Ref.
PPy nanowires	Chemical oxidation polymerization	221.7 ± 30.2	10.1 ± 0.1	(22.6 ± 3.6) × 10^{-3}	27
Free-standing PPy films	Interfacial chemical polymerization	162.7 × 10^2	4–8	0.45	44
PPy nanotube	Chemical oxidation polymerization	3382	12.76	0.55	45
PPy nanowire/rGO	Interfacial adsorption-soft template polymerization	75.1 × 10^2	33.8	8.56 ± 0.76	26
PPy/SWCNT	Physical mixing and vacuum filtration	~300 × 10^2	~25	21.7 ± 0.8	28
PPy/rGO	Template-directed *in situ* polymerization	41.6 × 10^2	26.9	3.01	25
PPy/silver nanocomposite	Photo-polymerization	11.87 × 10^2	6.85	0.056	23
PPy/MWCNTs (68 wt%)	*In situ* polymerization	35–40 × 10^2	24.4	2.2	46
PPy/SWCNTs	Interfacial polymerization	341.6 ± 4.7 × 10^2	33.2 ± 0.7	37.6 ± 2.3	This work

several order of magnitude higher to the reported values, including pure PPy film, PPy nanowires, PPy nanotube, and PPy based composites. The result indicates that design strategy proposed here is an effective way to enhance the TE properties and it can also be expanded to other conducting polymer based composite systems for higher TE performance.

Conclusions

In summary, high conductive PPy/SWCNTs composite films have been prepared by chemical interfacial polymerization under a controlled temperature. FESEM observation shows the smooth and compact structure of the interfacial polymerized PPy film. FTIR and Raman spectra indicate the high conjugation length and ordered molecular structure of the prepared PPy film, leading to the electrical conductivity of the PPy film can be as high as ~500 S cm^{-1}. The addition of SWCNTs play a key role to further enhance the Seebeck coefficient of the composite. Taking the advantage of the synergistic effect and the energy filtering effect between the PPy and SWCNTs, the power factor can be improve to 37.6 ± 2.3 μW mK^{-2}, which is 3 orders of magnitude higher than that of PPy power obtained by

traditional chemical oxidation polymerization. The present study indicates the promising candidate as organic TE materials for the high conductive PPy/SWCNTs composite films prepared by interfacial polymerization under a controlled temperature. Also, the design strategy in this study can be expanded to construct other conducting polymer based nanocomposite for higher TE performance.

Conflicts of interest

There are no conflicts to declare.

Acknowledgements

This work was supported by the Natural Science Foundation of Zhejiang Province (Grant No. LQ20E030015), Science and Technology Bureau Project of Jiaxing (Grant No. 2020AY10010), National Natural Science Foundation of China (Grant No. 51775242), and Research Training Program for College Students of Jiaxing University in 2020 (CD8517203214).

References

1 G. J. Snyder and E. S. Toberer, *Nat. Mater.*, 2008, **7**, 105–114.
2 K. Biswas, J. Q. He, I. D. Blum, C. I. Wu, T. P. Hogan, D. N. Seidman, V. P. Dravid and M. G. Kanatzidis, *Nature*, 2012, **489**, 414–418.
3 W. Jin, L. Liu, T. Yang, H. Shen, J. Zhu, W. Xu, S. Li, Q. Li, L. Chi, C.-A. Di and D. Zhu, *Nat. Commun.*, 2018, **9**, 3586.
4 X. Zhang and L. D. Zhao, *J. Materiomics*, 2015, **1**, 92–105.
5 W. Zhao, Z. Liu, Z. Sun, Q. Zhang, P. Wei, X. Mu, H. Zhou, C. Li, S. Ma, D. He, P. Ji, W. Zhu, X. Nie, X. Su, X. Tang, B. Shen, X. Dong, J. Yang, Y. Liu and J. Shi, *Nature*, 2017, **549**, 247–251.
6 L. Chen, X. Zhen and B. S. Qiang, *J. Inorg. Mater.*, 2010, **25**, 561–568.
7 L. Deng and G. Chen, *Nano Energy*, 2021, **80**, 105448.
8 K. Yusupov and A. Vomiero, *Adv. Funct. Mater.*, 2020, **30**, 2070342.
9 Y. Du, J. Xu, B. Paul and P. Eklund, *Appl. Mater. Today*, 2018, **12**, 366–388.
10 H. Song and K. Cai, *Energy*, 2017, **125**, 519–525.
11 O. Bubnova, Z. U. Khan, A. Malti, S. Braun, M. Fahlman, M. Berggren and X. Crispin, *Nat. Mater.*, 2011, **10**, 429–433.
12 H. Song, Q. Meng, Y. Lu and K. Cai, *Adv. Electron. Mater.*, 2019, 1800822.
13 L. Wang, Z. Zhang, Y. Liu, B. Wang, L. Fang, J. Qiu, K. Zhang and S. Wang, *Nat. Commun.*, 2018, **9**, 1–8.
14 C. Cho, B. Stevens, J.-H. Hsu, R. Bureau, D. A. Hagen, O. Regev, C. Yu and J. C. Grunlan, *Adv. Mater.*, 2015, **27**, 2996–3001.
15 L. Wang, Q. Yao, J. Xiao, K. Zeng, S. Qu, W. Shi, Q. Wang and L. Chen, *Chem.–Asian J.*, 2016, **11**, 1804–1810.
16 L. X. Wang, X.-G. Li and Y.-L. Yang, *React. Funct. Polym.*, 2001, **47**, 125–139.
17 J. Ouyang and Y. Li, *Polymer*, 1997, **38**, 3997–3999.
18 C.-E. Zhao, J. Wu, S. Kjelleberg, J. S. C. Loo and Q. Zhang, *Small*, 2015, **11**, 3440–3443.
19 X. Chen, D. M. Li, S. F. Liang, S. Zhan and M. Liu, *Sens. Actuators, B*, 2013, **177**, 364–369.
20 D. Wang, Y. X. Li, Z. Shi, H. L. Qin, L. Wang, X. F. Pei and J. A. Jin, *Langmuir*, 2010, **26**, 14405–14408.
21 J. Lei, Z. Li, X. Lu, W. Wang, X. Bian, T. Zheng, Y. Xue and C. Wang, *J. Colloid Interface Sci.*, 2011, **364**, 555–560.
22 U. Sree, Y. Yamamoto, B. Deore, H. Shiigi and T. Nagaoka, *Synth. Met.*, 2002, **131**, 161–165.
23 M. Bharti, A. Singh, S. Samanta, A. K. Debnath, D. K. Aswal, K. P. Muthe and S. C. Gadkari, *Energy Convers. Manage.*, 2017, **144**, 143–152.
24 J. Wang, K. Cai, S. Shen and J. Yin, *Synth. Met.*, 2014, **195**, 132–136.
25 S. Han, W. Zhai, G. Chen and X. Wang, *RSC Adv.*, 2014, **4**, 29281–29285.
26 Z. Zhang, G. Chen, H. Wang and W. Zhai, *J. Mater. Chem. C*, 2015, **3**, 1649–1654.
27 L. Liang, G. Chen and C. Y. Guo, *Mater. Chem. Front.*, 2017, **1**, 380–386.
28 L. Liang, G. Chen and C. Y. Guo, *Compos. Sci. Technol.*, 2016, **129**, 130–136.
29 G. Qi, L. Huang and H. Wang, *Chem. Commun.*, 2012, **48**, 8246–8248.
30 G. Qi, Z. Wu and H. Wang, *J. Mater. Chem. C*, 2013, **1**, 7102–7110.
31 J. Wang, K. Cai, J. Yin and S. Shen, *Synth. Met.*, 2017, **224**, 27–32.
32 H. Song, Y. Qiu, Y. Wang, K. Cai a, D. Li, Y. Deng and J. He, *Compos. Sci. Technol.*, 2017, **153**, 71–83.
33 C. Gao and G. Chen, *Compos. Sci. Technol.*, 2016, **124**, 52–70.
34 Y. Han, M. Shen, X. Lin, B. Ding, L. Zhang, H. Tong and X. Zhang, *Synth. Met.*, 2012, **162**, 753–758.
35 P. Xu, X. Han, C. Wang, D. Zhou, Z. Lv, A. Wen, X. Wang and B. Zhang, *J. Phys. Chem. B*, 2008, **112**, 10443–10448.
36 B. Tian and G. Zerbi, *J. Chem. Phys.*, 1990, **92**, 3886.
37 P. Jha, S. P. Koiry, V. Saxena, P. Veerender, A. K. Chauhan, D. K. Aswal and S. K. Gupta, *Macromolecules*, 2011, **44**, 4583–4585.
38 L. N. Fan and X. C. Xu, *Compos. Sci. Technol.*, 2015, **118**, 264–268.
39 L. Dauginet-De Pra and S. Demoustier-Champagne, *Polymer*, 2005, **46**, 1583–1594.
40 Z. Gu, C. Li, G. Wang, L. Zhang, X. Li, W. Wang and S. Jin, *J. Polym. Sci., Part B: Polym. Phys.*, 2010, **48**, 1329–1335.
41 Q. Yao, L. Chen, W. Zhang, S. Liufu and X. Chen, *ACS Nano*, 2010, **4**, 2445–2451.
42 D. H. Won, J. Chung, S. H. Park, E.-H. Kim and S. I. Woo, *J. Mater. Chem. A*, 2015, **3**, 1089–1095.
43 S. Suzuki, C. Bower, Y. Watanabe and O. Zhou, *Appl. Phys. Lett.*, 2000, **76**, 4007–4009.
44 M. Bharti, P. Jha, A. Singh, A. K. Chauhan, S. Misra, M. Yamazoe, A. K. Debnath, K. Marumoto, K. P. Muthe and D. K. Aswal, *Energy*, 2019, **176**, 853–860.
45 Y. Wang, Q. Yin, K. Du, S. Mo and Q. Yin, *Macromol. Res.*, 2020, **28**, 973–978.
46 H. Song, K. Cai, J. Wang and S. Shen, *Synth. Met.*, 2016, **211**, 58–65.